Comparison of WorldSID to PMHS kinematics in far-side impact

Daniel Perez-Rapela, Craig Markusic, Bryant Whitcomb, Bengt Pipkorn, Jason L. Forman, John-Paul Donlon, Salvador Montesinos Acosta, Jeff R. Crandall

Abstract Far-side impacts represent 9.5% of all automobile crashes and 8.3% of all MAIS3+ injuries. This type of event generates loads that challenge current restraint systems by setting the occupant on an inward motion. This complex motion, influenced by a number of restraint and impact parameters, often results in a loss of shoulder-to-belt contact. Reducing the negative outcomes of this type of crash requires an ATD capable of correctly representing the kinematics and sensitivity to restraint and impact parameters. The WorldSID is the most advanced ATD for injury evaluation in near-side crashes. However, its suitability for far-side scenarios still needs to be evaluated. This study performed a parametric evaluation of the effect of restraint and impact parameters on WorldSID kinematics. A total of 19 tests in six different test configurations were conducted, matching previously published PMHS tests. The ATD motion was tracked with a 3D high-speed motion-capture system. The parameters varied were: the impact severity and direction; D-ring position; pelvic restraint; and seat belt pretensioning. The ATD response and sensitivity to parameters were evaluated and compared to previously published PMHS data. The results show discrepancies in shoulder-belt engagement, head and torso kinematics and sensitivity to initial conditions.

Keywords WorldSID, far-side, biofidelity, corridors, sensitivity analysis.

I. INTRODUCTION

Far-side impacts represent 9.5% of all automobile crashes and 8.3% of all MAIS3+ injuries [1]. Numerous studies point to the head and thorax as the most commonly injured body regions [1–8], with a typical intrusion profile between 3 and 4 for AIS3+ injury severity, based on the SAE collision deformation standard [4][7]. Given that the leading cause of head injury is impact with the struck side of the vehicle [4], reducing vehicle intrusion and head excursion is crucial for injury prevention. The existing literature [9-10] shows increased head excursion in oblique cases when compared to purely lateral impacts. Complex shoulder mechanics related to loss of engagement with the shoulder-belt have been hypothesised to be the causes for this counterintuitive phenomenon [10].

Consumer groups and manufacturers are gaining interest in evaluating vehicle performance in this crash mode, but there is a lack of information regarding the performance of the anthropomorphic test devices (ATDs) in this loading configuration. Understanding the capabilities and limitations of these ATDs is key for the correct development and evaluation of far-side specific restraints.

The WorldSID is the most advanced ATD for injury evaluation in near-side crashes. However, its suitability for far-side scenarios needs to be further evaluated. The existing literature [9], based on individual PMHS responses, is insufficient to fully evaluate the WorldSID biofidelity. The present study compares the ATD head and torso kinematics to recently developed, unpublished PMHS far-side kinematic corridors based on [10]. In addition to the case-by-case kinematic comparison, this study also evaluates the biofidelity of the ATD sensitivity to parameters by comparing its performance to already published PMHS data [9-10].

D. Perez-Rapela (tel: +1-434-297-8070; e-mail: dp4db@virginia.edu) is a PhD Student, J. L. Forman is a Principal Scientist, J. P. Donlon is a Graduate Research Assistant, S. Montesinos Acosta is a Restraint Design and Testing Engineer and J. R. Crandall is a Professor of Mechanical and Aerospace Engineering, all at University of Virginia, USA. C. Markusic and B. Whitcomb are Principal Engineers at Honda R&D Americas, Inc. B. Pipkorn is Director of Simulation and Active Structures at Autoliv Research, Vårgårda, Sweden, and Adjunct Professor at Chalmers University of Technology in Gothenburg.

II. METHODS

For the present study, 19 sled tests were conducted with the WorldSID in six different impact configurations (TABLE I) selected from [10]. Variations in pulse intensity (34 km/h and 14 g, 16 km/h and 6.6 g), impact direction (oblique 60°, lateral 90°), D-ring location (forward, intermediate, back), pretensioner usage (yes, no) and additional pelvic restraint (yes, no) were studied. The low-severity sled pulse represents the median severity of far-side tow-away crashes. The high severity pulse represents the median severity at which MAIS3+ injuries occurred [4]. The pelvic restraint consists of a metal plate rigidly attached to the right-hand side of the seat. It was implemented into the test matrix to simulate the presence of a centre console.

TABLE I
IMPACT CONFIGURATIONS

Conf. #	ΔV (km/h)	Impact Direction	D-Ring Position	Pretensioner	Pelvic restraint
1	16	Oblique	Intermediate	No	No
2	16	Oblique	Intermediate	Yes	No
3	34	Oblique	Intermediate	Yes	No
4	16	Oblique	Back	Yes	Yes
5	16	Lateral	Forward	Yes	No
6	34	Lateral	Intermediate	Yes	No

The tests were conducted on the same sled, sled fixture and restraint systems as the PMHS tests presented in [10]. The sled fixture was designed to approximate a vehicle-based restraint environment while providing repeatable and reproducible test conditions and lines of sight for motion capture. The seat consisted of an aluminium plate mounted on top of a six-axis load cell, covered by a 6.25 mm layer of neoprene rubber (durometer value 30A). The seatback consisted of two horizontal aluminium bars whose position could be adjusted in the anterior-posterior and superior-inferior directions to produce the desired postures (Fig. 1). The seat and seatback were instrumented with single-axis accelerometers oriented with the principal direction of force (PDOF). The restraint system consisted of a 3-point seat-belt with optional pretensioner and a 4 kN–2.5 kN degressive load limiter. The shoulder- and lap-belt tension were tracked using four Messring 15 kN seat-belt load cells. The retractor was mounted on a six-axis load cell to verify the accuracy of the seat-belt load cells.

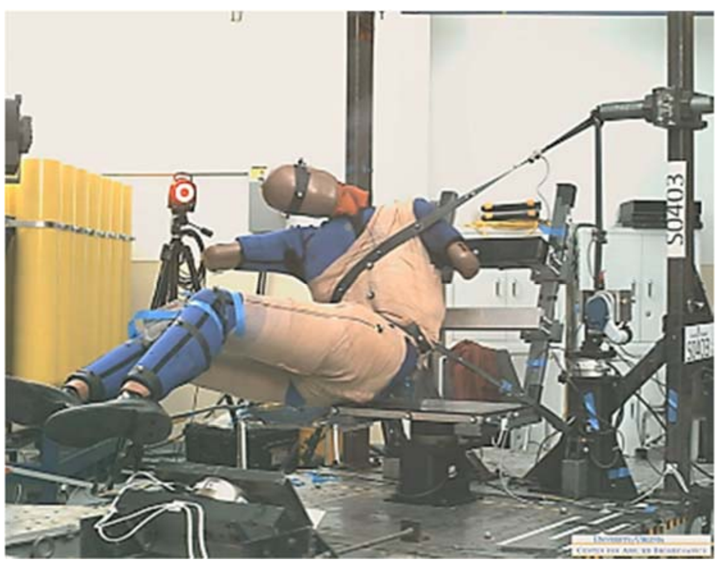

Fig. 1. Test fixture.

The ATD was positioned to match the average PMHS pelvic position, pelvis-to-shoulder angle and shoulder to D-ring vector for each D-ring position. The ATD was instrumented with its standard sensors, including linear accelerometers and angular velocity sensors for the head, T12 and pelvis. The rib deflection was measured by 2D-IRTRACC and RibEye technology in paired tests. The ATD kinematic data were captured using a 500-Hz Vicon MX™ three-dimensional (3D), camera-based motion capture system, and three high-speed video cameras. Vicon markers were located on the ATD's surface for point tracking on shoulders, arms, legs and torso. Head, T1 and pelvis position and orientation were tracked by placing an array of markers.

Given that the WorldSID neck implements some degree of passive muscle response, this study focuses not only on the head but also on torso kinematics. These kinematics account for head and T1 forward and lateral excursion and left shoulder forward excursion with respect to the sled. The latter is particularly important for analysing shoulder-to-belt interaction. The resultant responses were evaluated and compared to the existing WorldSID and PMHS data.

Corridor comparison

PMHS corridors were developed for the configurations of interest (TABLE I) based on previously published data [10]. Corridors for configurations informed by multiple PMHS tests were developed using the corresponding PMHS mean response and variance. Corridors for configurations informed by a single PMHS test (configurations 4 and 6) were developed by using the individual PMHS response and the variance observed in similar test configurations. Information about their development can be found in Appendix A.

The resulting WorldSID head and torso kinematics were compared to the PMHS corridors. The ATD biofidelity was evaluated using a correlation and analysis (CORA) method [11]. The CORA method assigns a correlation score between the ATD and the PMHS responses by applying two methods: the corridor method, and the cross-correlation method. The corridor method analyses the fitting of the response into the PMHS corridor. The cross-correlation method compares the phase, shape and area below the ATD and PMHS responses. The final CORA score is calculated as a weighted average of the two methods:

$$CORA_{Score} = 0.5 \cdot Score_{corridor} + 0.5 \cdot (0.5 \cdot Score_{shape} + 0.25 \cdot Score_{phase} + 0.25 \cdot Score_{area})$$

Sensitivity to parameters

A linear regression model was calculated based on the ATD results. The sensitivity to the different test parameters (not including the pelvic restraint) was evaluated and compared to previously published PMHS data [9-10].

III. RESULTS

Corridor comparison

This section shows the kinematic results for head and torso, along with their corresponding CORA score (in parentheses). A complete corridor comparison can be found in Appendix B. The corresponding video images can be found in Appendix C.

Configuration 1 consists of a low intensity pulse at 60° without pretensioner. The results for this configuration (Fig. 2) show good agreement between the WorldSID and PMHS lateral excursion for both head and torso. The forward excursion shows less agreement between the surrogates, especially in the head where the ATD exhibits a premature and more aggressive rebound.

The ATD shoulder forward excursion is similar to the PMHS up to around 60 ms, where the ATD reaches its maximum forward excursion.

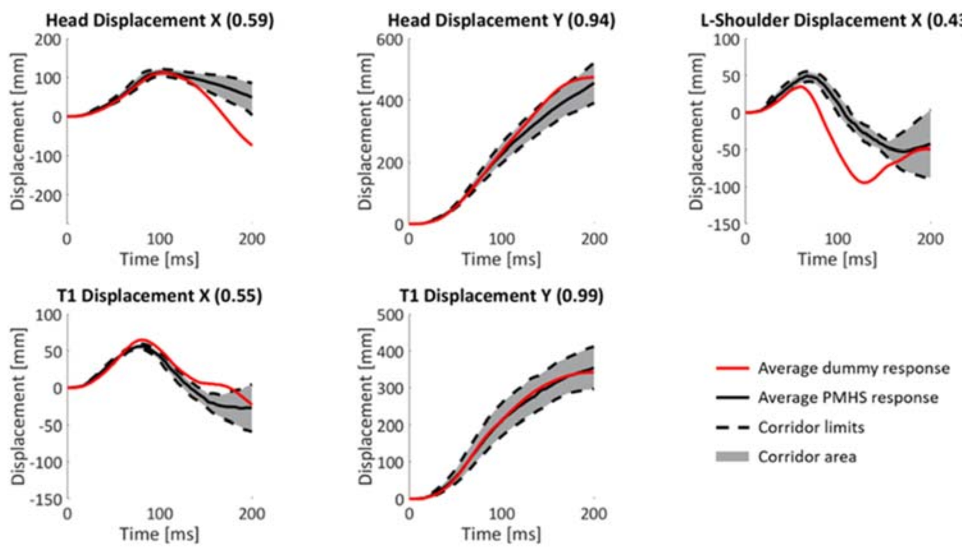

Fig. 2. Head and torso kinematics in configuration 1.

Configuration 2 differs from configuration 1 in the usage of the pretensioner. The results for this configuration (Fig. 3) show a biofidelic lateral head and T1 excursion. The longitudinal excursion is correctly captured by T1. However, the head exhibits less forward excursion than the PMHS, with an associated CORA score of 0.28.

The WorldSID shoulder exhibits increased rearward kinematics when compared to the PMHS. This is particularly true for the first 100 ms.

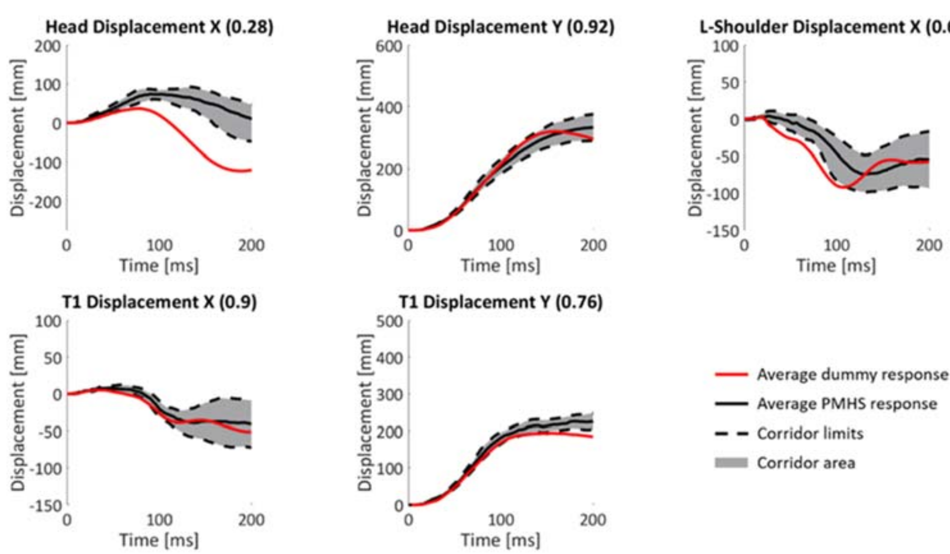

Fig. 3. Head and torso kinematics in configuration 2.

Configuration 3 differs from configuration 2 in the pulse intensity. The ATD exhibits reduced forward and lateral excursion in this configuration (Fig. 4). Only the lateral head excursion reaches the PMHS maximum value, but it springs back sooner, achieving a CORA score of 0.64.

Shoulder kinematics are particularly non-biofidelic in this configuration. The PMHS exhibits an initial forward excursion followed by a progressive rearward excursion halfway through the event. On the other hand, the WorldSID shoulder moves rearwards after a very limited forward excursion. The shoulder kinematics have an associated CORA score of 0.35.

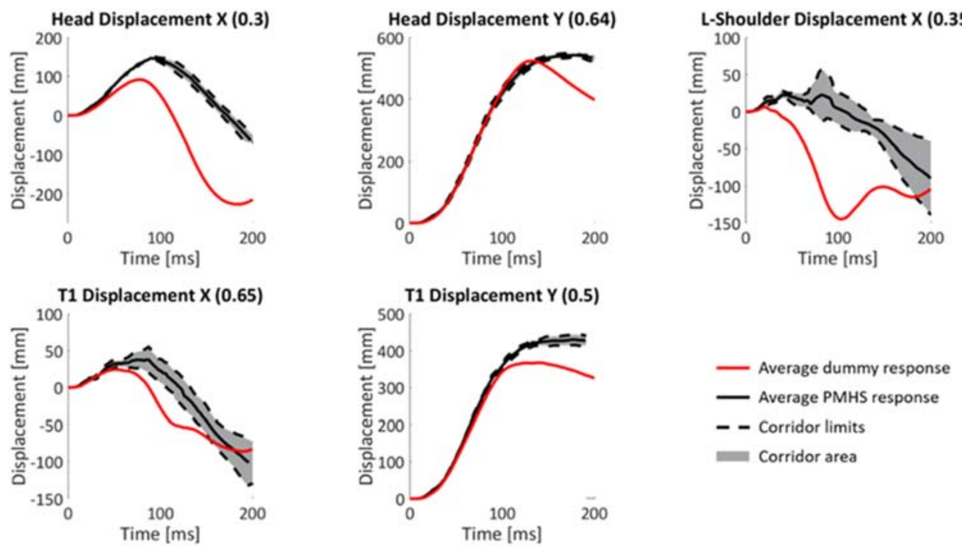

Fig. 4. Head and torso kinematics in configuration 3.

The WorldSID exhibits reduced lateral excursion in configuration 4. The addition of the pelvic restraint has a greater effect on the ATD than on the PMHS. Head and torso lateral excursions are underestimated. Head and torso forward excursion remains close to the PMHS corridor boundaries.

The ATD shoulder kinematics are very similar to configuration 2, with increased rearward motion until 100 ms.

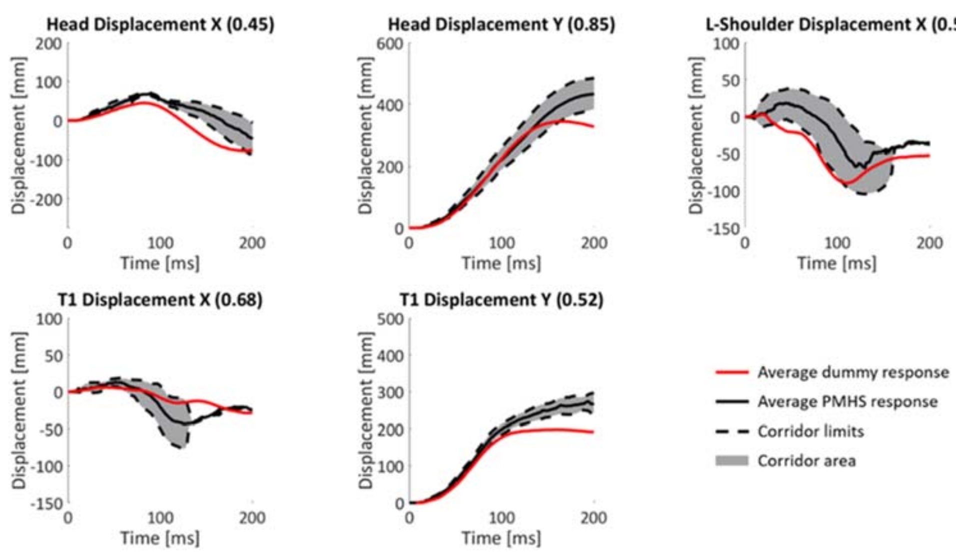

Fig. 5. Head and torso kinematics in configuration 4.

The WorldSID exhibits biofidelic forward excursion for the head and torso and slightly increased lateral kinematics when compared to the PMHS in 90° cases (

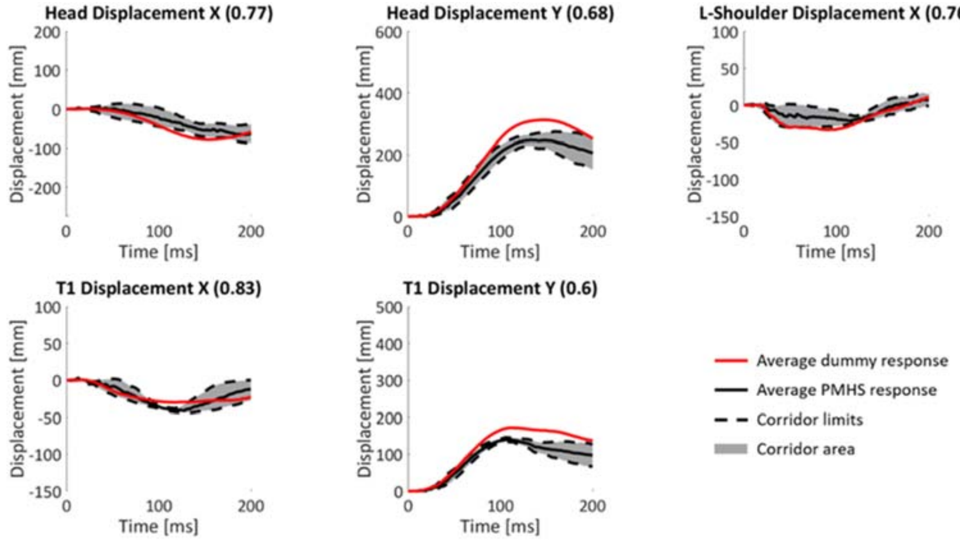

Fig. **6** and Fig. Fig. **7**).

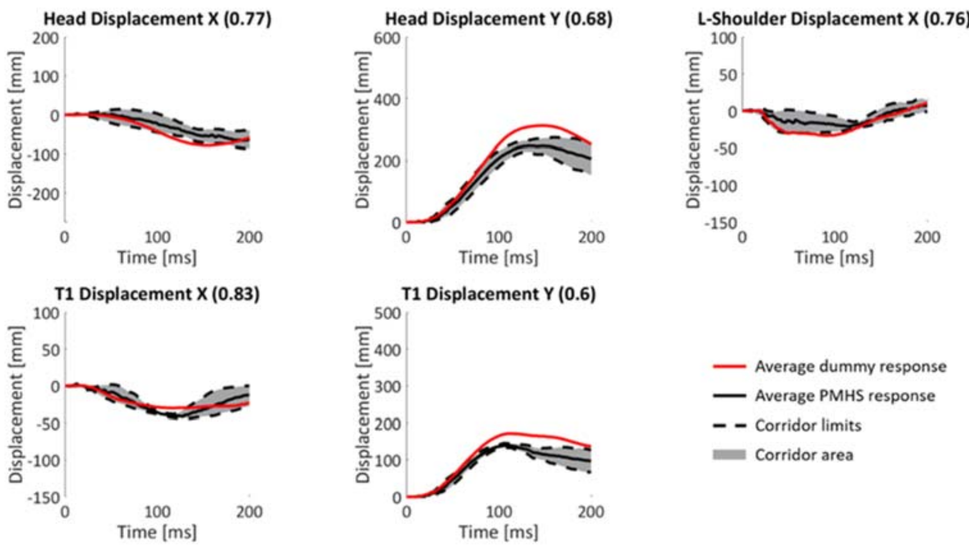

Fig. 6. Head and torso kinematics in configuration 5.

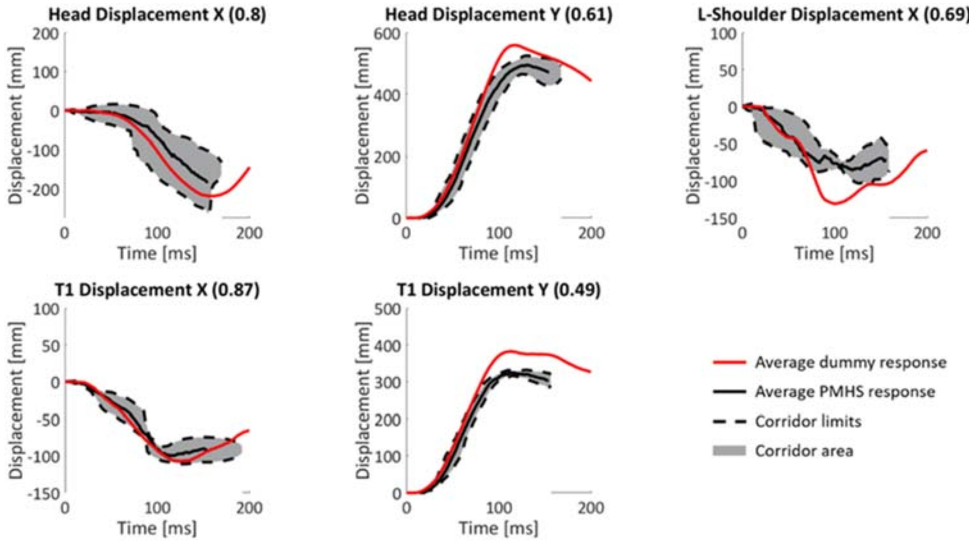

Fig. 7. Head and torso kinematics in configuration 6.

TABLE II shows a summary, with the CORA scores achieved for each configuration and body region. Given that there are no categories associated with specific CORA scores, the evaluation is limited to relative comparisons rather than absolute assessments.

The configuration associated with the worst overall CORA score is configuration 3. In the 90° cases, the worst performing configuration is also the one with the highest severity pulse. In general, lateral head excursions are associated with a higher CORA score than longitudinal excursions. The opposite is true for T1. Head exhibits better performance than T1 in lateral excursion, but the opposite is true for longitudinal excursion. The head and shoulder are the worst performing body regions for the 60° cases.

TABLE II
CORA SCORES

Conf. #	**Head**		**T1**		**Shoulder**	**Average per configuration**
	Long.	Lat.	Long.	Lat.	Long.	
1	0.59	0.94	0.55	0.99	0.42	0.70
2	0.28	0.92	0.9	0.75	0.68	0.71
3	0.30	0.64	0.65	0.5	0.35	**0.49**
4	0.44	0.85	0.68	0.52	0.5	0.60
Average per body motion PDOF = 60°	**0.40**	**0.84**	0.70	0.69	**0.49**	0.62
5	0.77	0.68	0.83	0.6	0.76	0.73
6	0.8	0.61	0.87	0.49	0.69	0.69
Average per body motion PDOF = 90°	0.79	0.65	0.85	0.55	0.73	0.71
Average per body motion	**0.53**	0.77	0.75	0.64	**0.57**	0.65

Sensitivity to parameters

TABLE III summarises the regression model created for the WorldSID lateral head excursion with respect to the sled pulse, impact direction, D-ring position and pretensioner usage. Based on this analysis, the WorldSID lateral head excursion significantly increases with the pulse intensity and decreases with the usage of a pretensioner. The usage of the pretensioner is associated with a reduction of 155.3 mm on head excursion. On the other hand, an increment on the impact direction, although not significant, shows an increase on head kinematics. That is, the lateral head excursion tends to be 34.62 mm larger on purely lateral events than on oblique events.

TABLE III
HEAD LATERAL DISPLACEMENT (MM)

Predictor		**Coefficient**	**SE Coefficient**	**p**
Constant		246.9	44.7	0.000
Pulse (g)		**27.73**	1.95	**0.000**
Impact direction (deg.)		**1.154**	0.76	0.153
D-Ring*	forward	-65.4	28.8	0.041
	intermediate	-24.1	14.4	0.118
Pretensioner**		**-155.3**	14.4	**0.000**
R^2 = 96.75%; Adjusted R^2 = 95.50%				

*Discrete predictor. **Dichotomous variable: No=0, Yes=1

IV. Discussion

Corridor comparison

Different field studies show that the head and thorax are the most commonly injured body regions [1][3–8][12]. Capturing the kinematics associated with these body regions is therefore critical for the correct analysis and optimisation of far-side specific countermeasures. Head and thorax kinematics have been associated with complex shoulder kinematics, more specifically with shoulder-to-belt interaction [10]. That is, capturing correct shoulder-to-belt interactions is key to capturing head and thorax kinematics.

The WorldSID shows fair shoulder biofidelity for the purely lateral cases, but limited biofidelity for the oblique cases. This is noticeable in all the cases, but especially in the high intensity pulse case (Fig. 4 and Fig. 8). Since this pulse represents the median severity at which MAIS3+ injuries occur [4], the lack of shoulder biofidelity limits the ability of the WorldSID to correctly represent human-to-belt interactions in injurious scenarios. This can have important consequences for restraint optimisation.

The WorldSID shows a clear lack of anterior-posterior chest deflection, which, in combination with the lack of shoulder motion, limits the ability of the ATD to correctly engage the shoulder-belt (Appendix C). This is especially noticeable in the cases with a pretensioner. In these cases, the PMHS chest deforms around the shoulder-belt while the ATD torso tends to rotate out of the seat-belt. This behaviour is a consequence of the ATD upper body construction whose main design focus was to represent human response in purely lateral, near-side events.

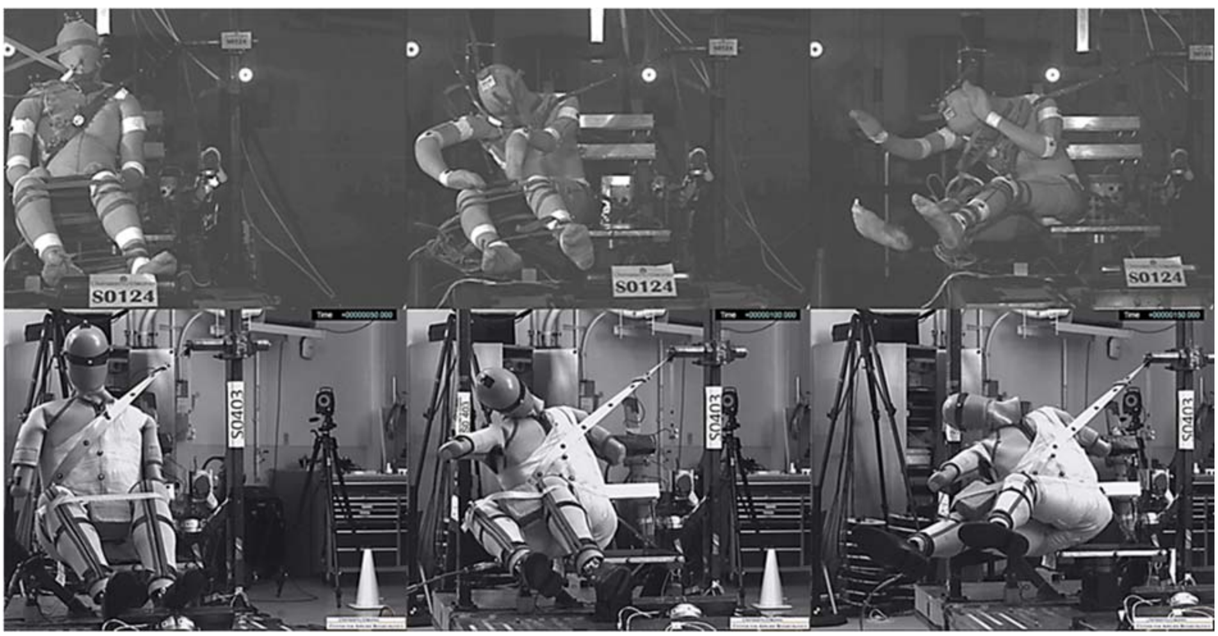

Fig. 8. WorldSID vs PMHS comparison in oblique high-speed impacts (configuration 3) at 50 ms (left), 100 ms (centre) and 150 ms (right).

The WorldSID lateral head excursion is generally associated with good peak and CORA values in the 60° cases. However, it shows reduced lateral excursion in the presence of the pelvic restraint. This may indicate that the WorldSID is not able to biofidelically represent the PMHS response to various degrees of pelvic restraint.

Although lateral head excursion seems to be relatively well represented, the WorldSID shows limitations in overall head kinematics. The lack of head forward excursion is especially concerning. Since the probability of hitting an intruding object increases with the area covered by the occupant's body, underestimating forward head excursion can limit the ability of the ATD to identify potential intruding hazards. Moreover, non-biofidelic forward motion can also limit the ability of the WorldSID to correctly assess the effectiveness of far-side specific restraint systems.

Head motion biofidelity is also limited by the kinematic biofidelity of the adjacent body regions. Therefore, although the WorldSID shows good lateral head excursion peaks in some cases, the lack of biofidelity of its torso indicates that lateral head excursions are circumstantially correct, but not necessarily biofidelically correct.

Due to lack of PMHS data, corridors for configurations 4 and 6 were developed based on single PMHS responses and the variance obtained from similar load cases. This technique allows for corridor estimation in cases with a single PMHS response. Although these corridors should be considered approximations, they provide a valid statistical base for assessing ATD responses.

Although the large motions imposed by this testing fixture help highlight the surrogate deficiencies, some of the resulting kinematics may be too extreme for a more vehicle-like environment. Therefore, some of the discrepancies found in this study may be reduced in a more vehicle-like environment. Further evaluations are needed to determine the response of the WorldSID to various degrees of lower body restraint.

Sensitivity to parameters

Traditional methods for the biofidelity evaluation of human surrogates consist mainly of corridor comparisons. This approach focuses on case-by-case analysis, but is limited in its ability to capture surrogate sensitivity to parameters. The present sensitivity analysis does not focus on comparing total head excursion, but rather on comparing its dependency to each testing parameter. Since we only evaluate the effect of each individual parameter and not the total quantitative excursion results, this method allows researchers to extract conclusions from test series with different excursion ranges.

According to the existing literature [9-10], PMHS show significant sensitivity to changes in pulse, pretensioning and PDOF. The regression analysis performed on the dummy results shows that the WorldSID exhibits correct sensitivity to pulse intensity and pretensioner usage. However, the ATD shows the opposite sensitivity to changes in PDOF when compared to the PMHS. The PMHS exhibit significantly larger head excursions in the oblique configurations, while the ATD shows larger excursions in purely lateral pulses. This is very likely related to a lack of chest deflection and shoulder and spine motion in the ATD.

A more in-depth biofidelity evaluation is not possible without a correct estimation of the effect of the PMHS variability on the overall kinematics. Parameters like body height, mass or shape could not be taken into account in the original PMHS evaluation. Further work is needed to fully understand the contribution these different factors have on human kinematics.

V. CONCLUSIONS

The present kinematic biofidelity evaluation focuses on WorldSID head and torso kinematics.

WorldSID and PMHS exhibit similar sensitivity to pulse intensity and pretensioner use. However, the ATD shows the opposite sensitivity to changes in the impact direction when compared to the PMHS.

Peak lateral head excursion is generally similar to that of the PMHS for the 60° cases. However, the ATD shows reduced head excursion in the presence of a pelvic restraint and slightly increased head excursion in the 90° cases.

The ATD consistently underestimates PMHS forward head excursion for the 60° cases.

The ATD shoulder motion and shoulder-to-belt interaction do not represent PMHS kinematics.

Future work includes the evaluation of the WorldSID biofidelity in vehicle-like environments and the evaluation of computational surrogates to fully understand the effect of human variability in the overall kinematic response.

VI. ACKNOWLEDGEMENTS

Jason Forman first suggested the idea to calculate n=1 corridors from similar n>1 corridors; Tim McMurray suggested how best to do so. Hamed Joodaki both originated and implemented a process to calculate corridor bounds from sets of ellipses, and Jacek Toczyski provided advice and instruction in previous corridor calculation methods. Tim Gillispie reviewed the grammar in this manuscript.

VII. REFERENCES

[1] Bahouth, G. T., Murakhovskiy, D., Digges, K. H., Rist, H., Wiik, R. (2015) Opportunities for reducing far-side casualties. *24th International Technical Conference on the Enhanced Safety of Vehicles (ESV)*, 2015, Gothenburg, Sweden, National Highway Traffic Safety Administration.

[2] Mackay, G. M., Hill, J., Parkin, S., Munns, J. A. R. (1993) Restrained occupants on the nonstruck side in lateral collisions. *Accident Analysis & Prevention*, **25**(2): pp.147–152.

[3] Frampton, R., Welsh, R., Thomas, P., Fay, P. (2000) The Importance of Non-struck Side Occupants in Side Collisions. *Journal of Crash Prevention and Injury Control*, **2**(2): pp.151–163.

[4] Gabler, H. C., *et al.* (2005) Far-side impact injury risk for belted occupants in Australia and the United States. *Proceedings of the 19th International Conference on Enhanced Safety of Vehicles*, 2005, Washington DC, USA.

[5] Ryb, G. E., *et al*. (2009) Expected Differences and Unexpected Commonalities in Mortality, Injury Severity, and Injury Patterns Between Near Versus Far Occupants of Side Impact Crashes. *The Journal of Trauma: Injury, Infection, and Critical Care*, **66**(2): pp.499–503.

[6] Viano, D. C., Parenteau, C. S. (2010) Severe Injury to Near- and Far-Seated Occupants in Side Impacts by Crash Severity and Belt Use. *Traffic Injury Prevention*, **11**(1): pp.69–78.

[7] Yoganandan, N., *et al*. (2014) Crash Characteristics and Injury Patterns of Restrained Front Seat Occupants in Far-side Impacts. *Traffic Injury Prevention*, **15**(sup1): S27–S34.

[8] Brumbelow, M. L., Mueller, B. C., Arbelaez, R. A. (2015) Occurrence of Serious Injury in Real-World Side Impacts of Vehicles with Good Side-Impact Protection Ratings. *Traffic Injury Prevention*, **16**(sup1): S125–S132.

[9] Pintar, F. A., *et al*. (2007) Comparison of PMHS, WorldSID, and THOR-NT responses in simulated far side impact. *Stapp Car Crash Journal*, **51**:313.

[10] Forman, J. L., *et al*. (2013) Occupant kinematics and shoulder belt retention in far-side lateral and oblique collisions: a parametric study. SAE Technical Paper, 2013.

[11] Gehre, C., Gades, H., Wernicke, P. (2009) Objective Rating of Signals Using Test and Simulation Responses. *Proceedings: International Technical Conference on the Enhanced Safety of Vehicles*, 2009, Stuttgart, Germany.

[12] Mackay, G.M., *et al*. (1993) Restrained occupants on the nonstruck side in lateral collisions. *Accident Analysis & Prevention*, **25**(2), pp.147-152.

[13] Lessley, D., Crandall, J., Shaw, G., Kent, R., Funk, J. (2004) A normalization technique for developing corridors from individual subject responses. SAE Technical paper, 2004.

[14] Shaw, J. M., Herriott, R. G., McFadden, J. D., Donnelly, B. R., Bolte, J. H. (2006) Oblique and lateral impact response of the PMHS thorax. SAE Technical Paper, 2006.

VIII. APPENDIX A

Introduction

This method elaborates previous techniques by Lessley *et al*. [13] and Shaw *et al*. [14]. The main characteristic of these techniques is the parametrisation of the response. This approach is adopted to better account for possible differences in time-to-peak in the individual responses.

Corridor Calculation

First, parametrise each curve by its arc-length, with the arc-length along the curve normalised based on the arc-length between two characteristic points on the curve (e.g. from the value at time 0 ms to the peak value, Fig. A-1, a and b). Second, calculate the mean and standard deviation in each axis (e.g. time and displacement) for each step in arc-length (Fig. A-1, c and d). Third, define the corridor as the set of ellipses with centres at each step in arc-length along the mean curve and semi-axes proportional to the standard deviation in each axis at each step in arc-length (Fig. A-1, e and f).

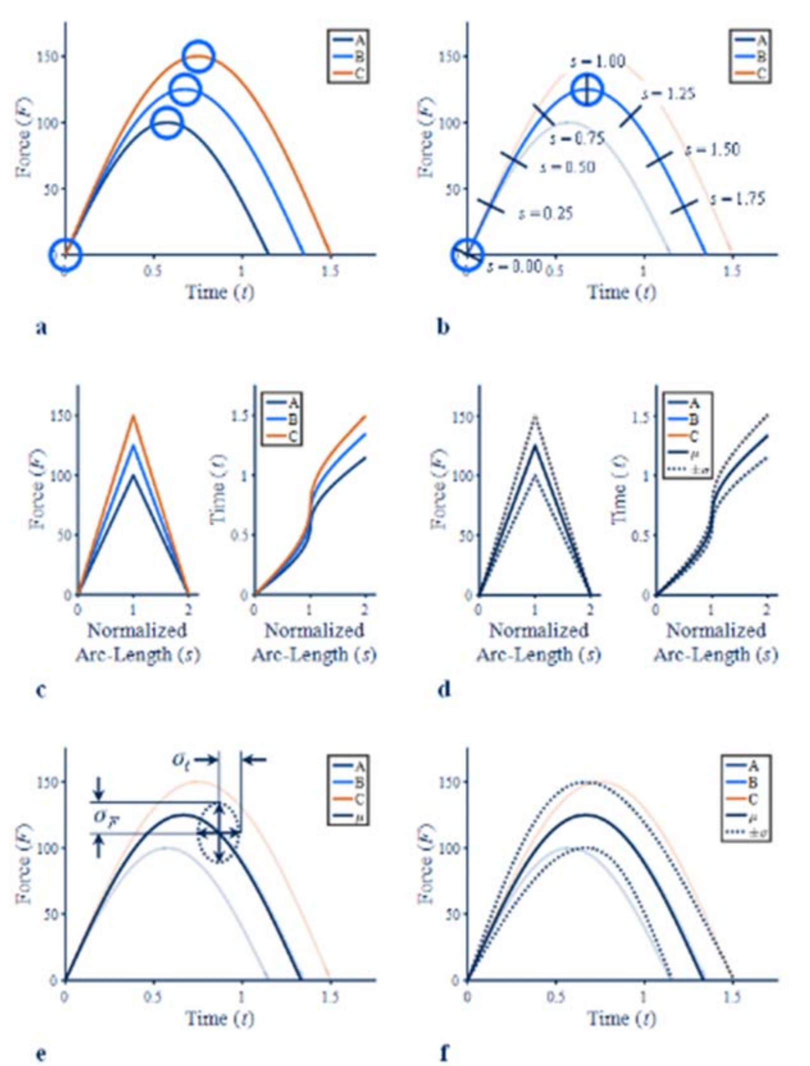

Fig. A-1.Illustration of parametrisation (a, b, c) and corridor creation (d, e, f) for an example data set (individual force time-histories A, B and C). The mean (μ) and standard deviation (σ) were calculated for force (F) and time (t) separately as functions of normalised arc-length (s).

Corridor Calculation Method for Single-Sample Tests

For a given test condition (*A*) with n>1 cadavers, we can create a *confidence interval* (corridor) using the mean and some multiple of the standard error (SE_A) of the individual responses. We can also calculate the sample standard deviation (s) of the individual responses, where $SE_A = s/\sqrt{n}$.

For a similar test condition (*B*) with n=1 cadaver (whether or not that same cadaver was tested in test condition (*A*)), we can create a *confidence interval* (corridor) using the cadaver's response and some multiple of the square root of the sum of the squared standard error and squared sample standard deviation from test condition (*A*), i.e. $SE_B = \sqrt{s^2 + SE_A^2} = \sqrt{s^2 + s^2/n} = s\sqrt{1 + 1/n}$.

For the present study, the n>1 and n=1 tests (with associated most similar tests) are listed in TABLE A **I** and TABLE A-II. Most similar test conditions to the n=1 tests were selected based on available n>1 tests and identical parameters (e.g. acceleration, principal degree of force) in as many ways as possible and ordered according to the sensitivity analysis of Forman *et al*. (2013) [10].

TABLE A I

TESTS UTILIZED IN CORRIDOR GENERATION (N>1)

Condition Code*	**Tests**
14/O/T/I/Yes/No	124, 135
6.6/O/T/I/No/No	122, 133, 136
6.6/O/T/I/Yes/No	123, 134, 137
6.6/L/T/F/Yes/No	83, 88
6.6/O/T/B/Yes/No	127, 132, 139

TABLE A-II

TESTS UTILIZED IN CORRIDOR GENERATION (N=1)

Condition Code*	**Test**	**Closest Condition**	**Closest Tests**
6.6/O/T/B/Yes/Yes	129	6.6/O/T/B/Yes/No	127, 132, 139
14/L/T/I/Yes/No	91	6.6/L/T/F/Yes/No	83, 88

*Condition code: Pulse (g) / Direction / Arm Position / D-Ring Position / Pretensioner / Pelvis Block
Direction: L=Lateral, O=Oblique; Arm Position: T=On Thighs, K=On Knees, U=Up
D-Ring Position: B=Back, I=Intermediate, F=Forward

IX. APPENDIX B

This appendix contains the WorldSID head, T1, pelvis excursion and seat-belt forces (red) and the corresponding PMHS corridors (shaded) for each test configuration.

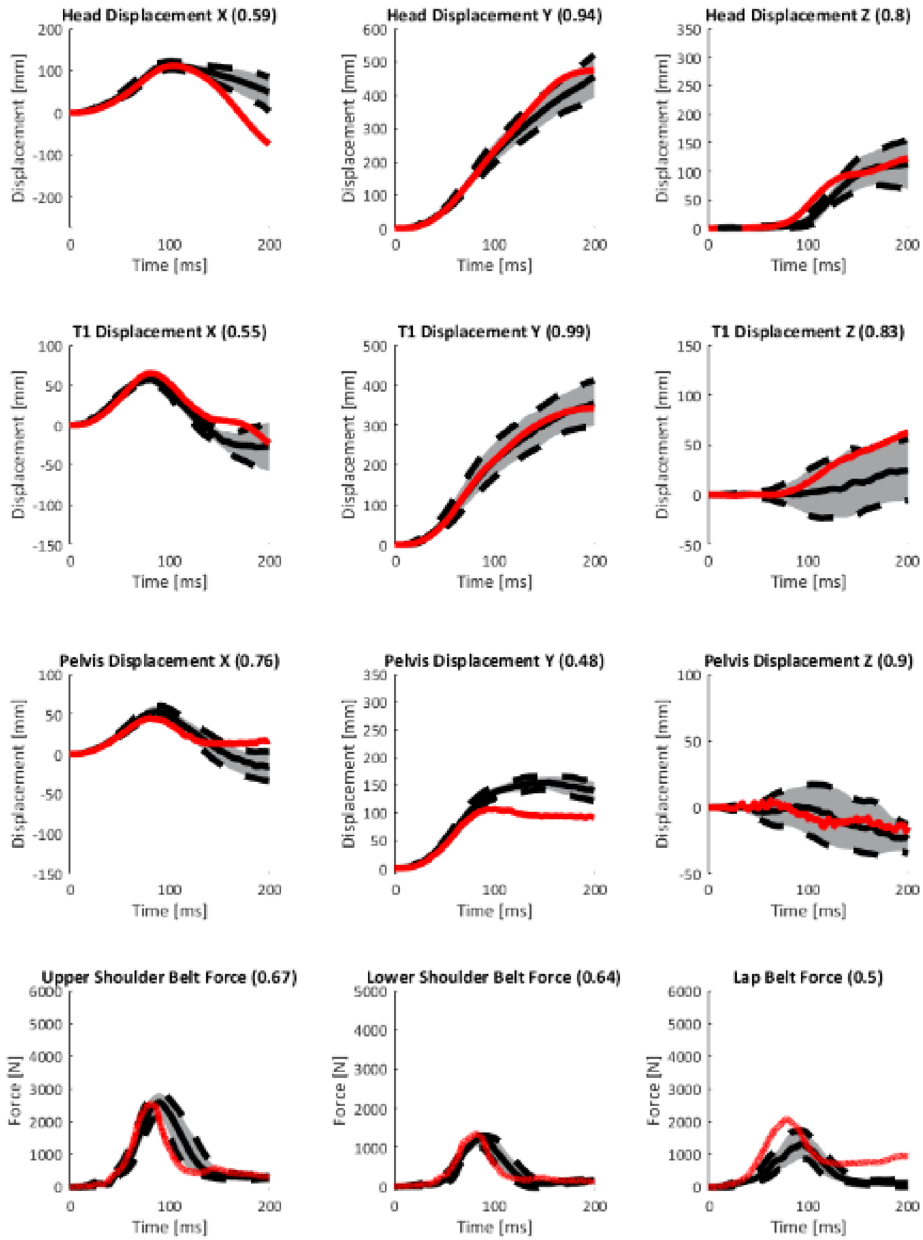

Fig. B-1. WorldSID and PMHS excursions and seat-belt forcer for configuration 1.

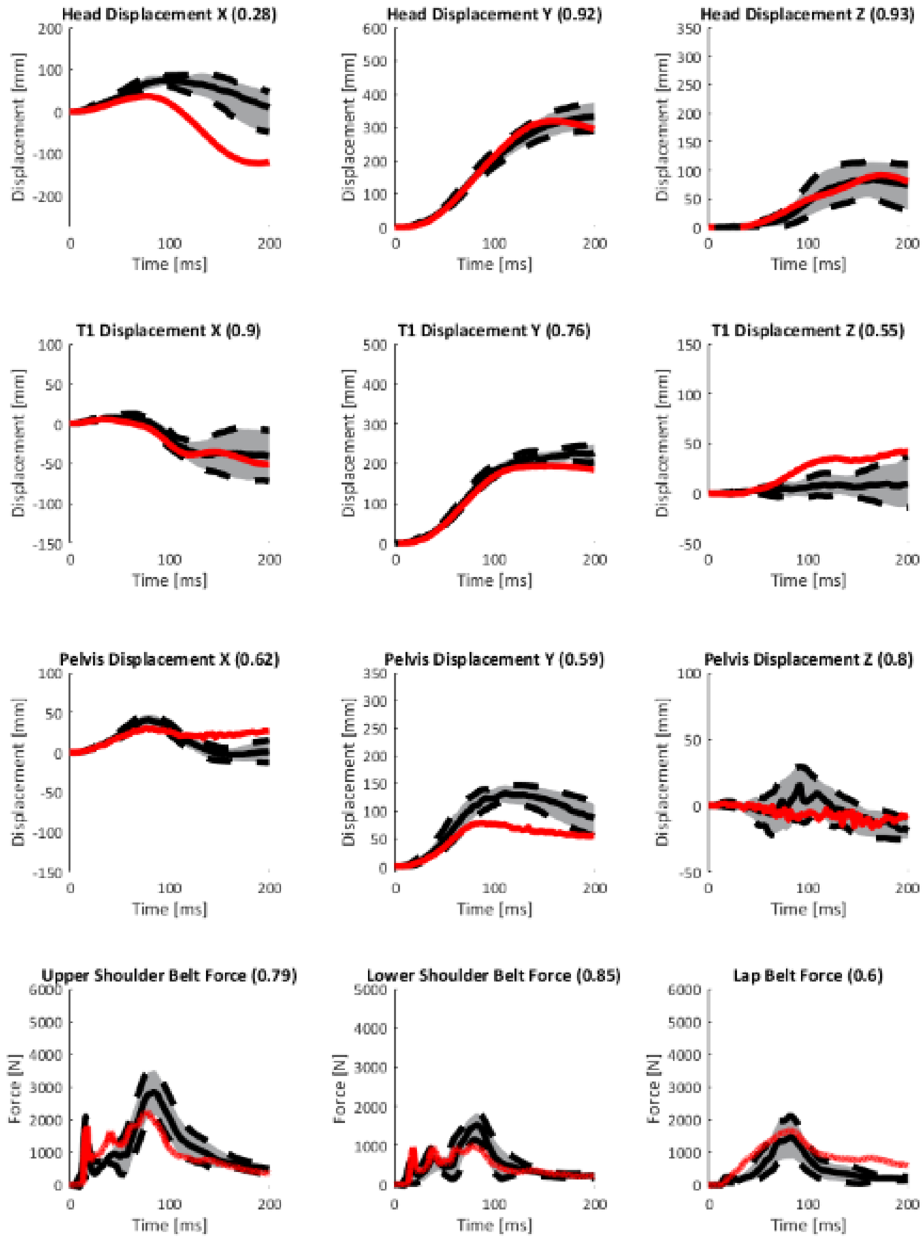

Fig. B-2. WorldSID and PMHS excursions and seat-belt forcer for configuration 2.

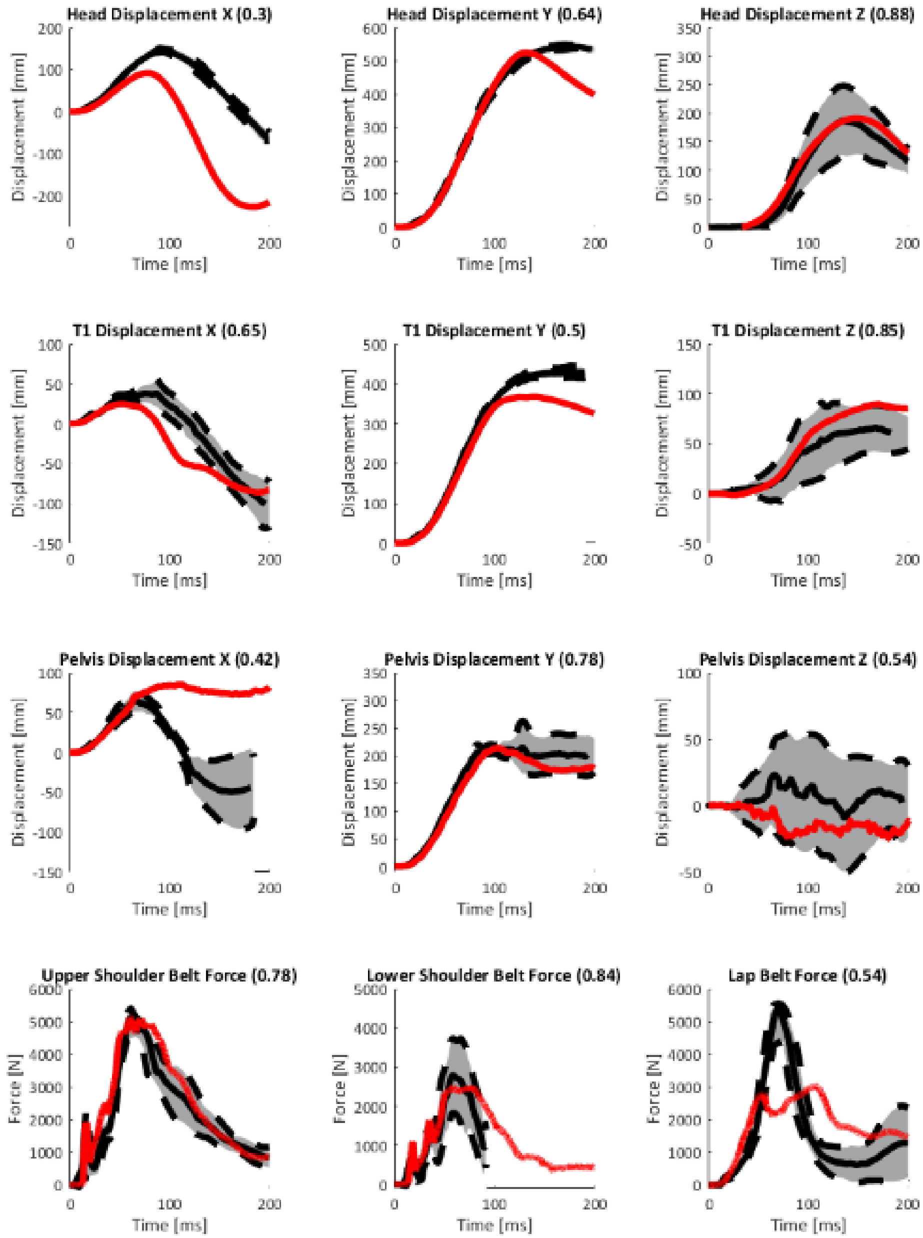

Fig. B-3. WorldSID and PMHS excursions and seat-belt forcer for configuration 3.

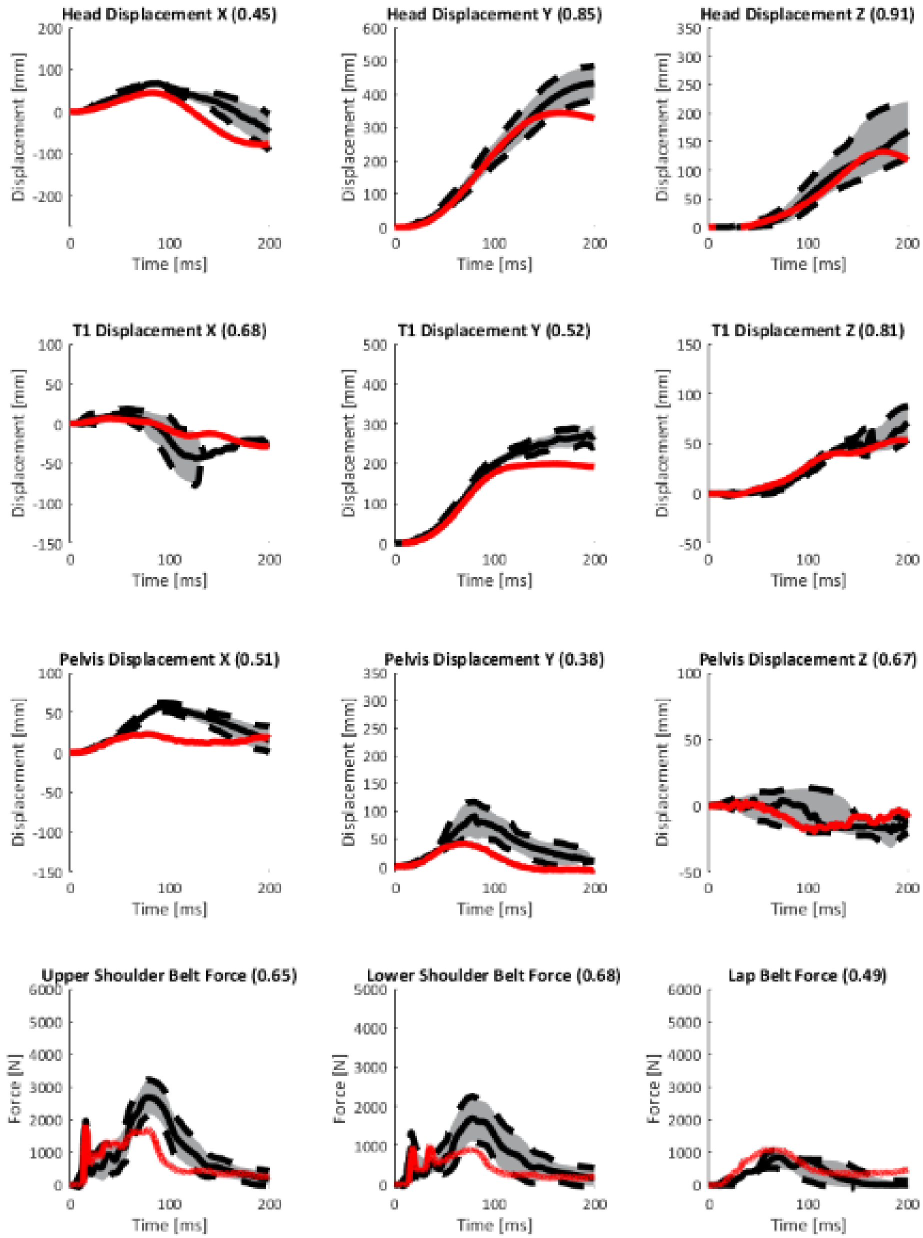

Fig. B-4. WorldSID and PMHS excursions and seat-belt forcer for configuration 4.

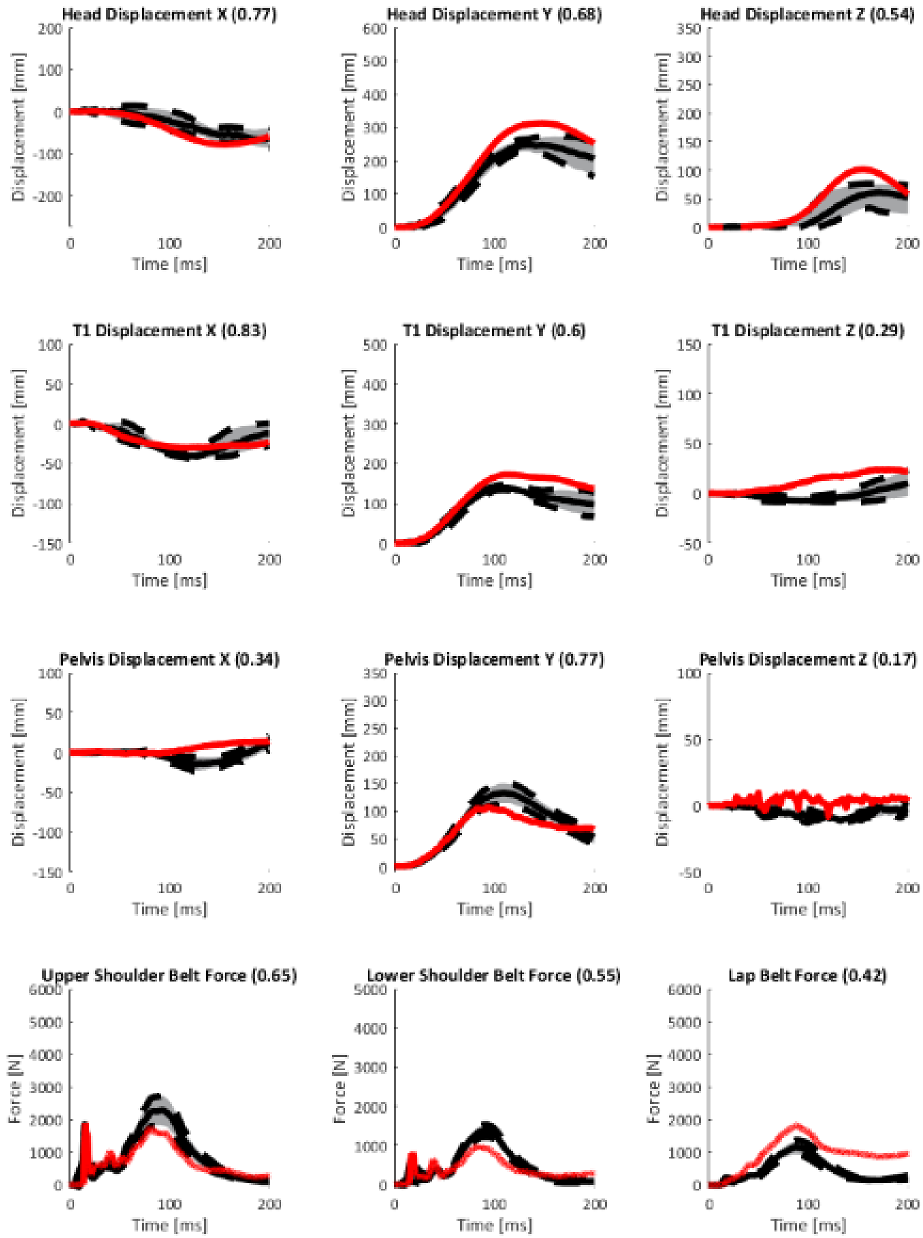

Fig. B-5. WorldSID and PMHS excursions and seat-belt forcer for configuration 5.

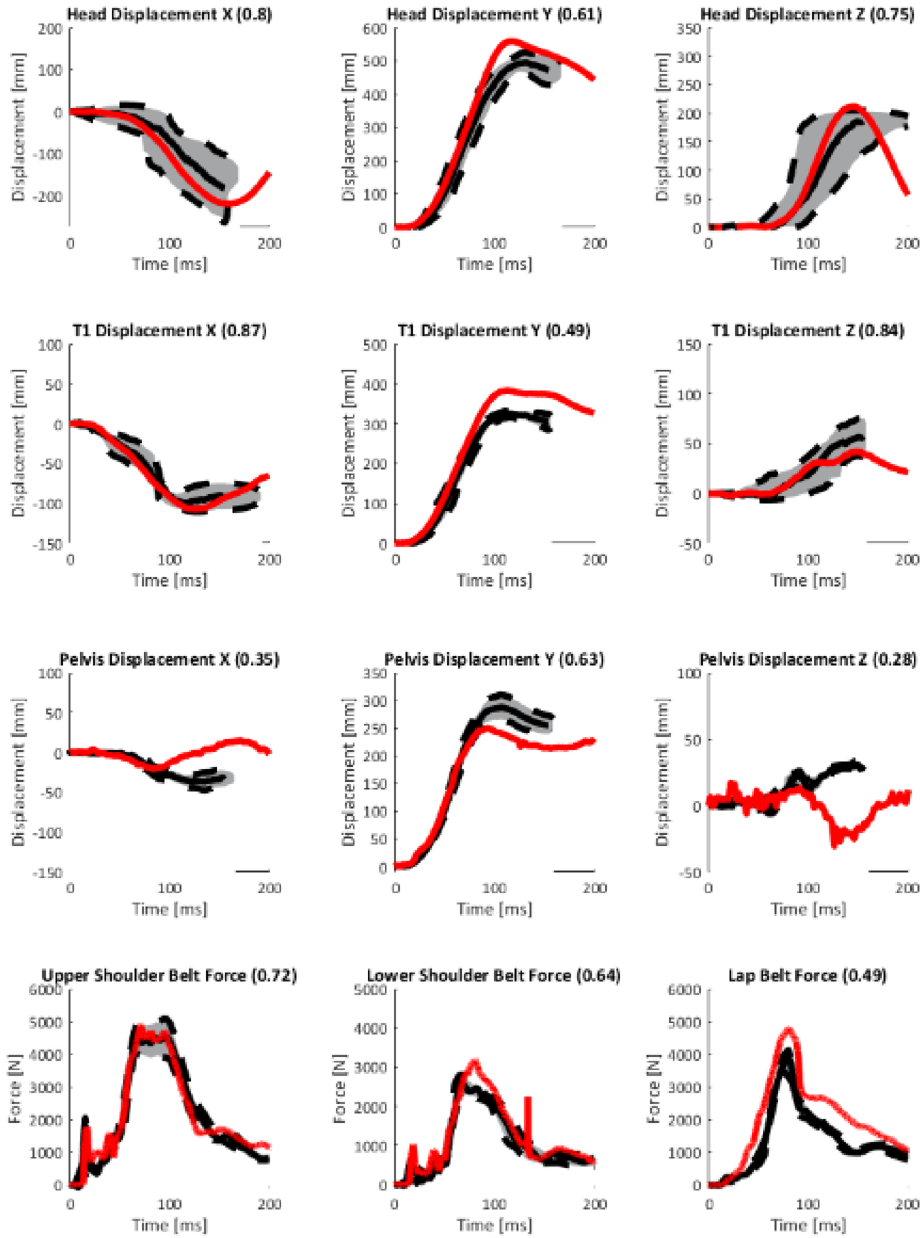

Fig. B-6. WorldSID and PMHS excursions and seat-belt forcer for configuration 6.

X. Appendix C

This appendix contains the frontal camera views for the different test configurations.

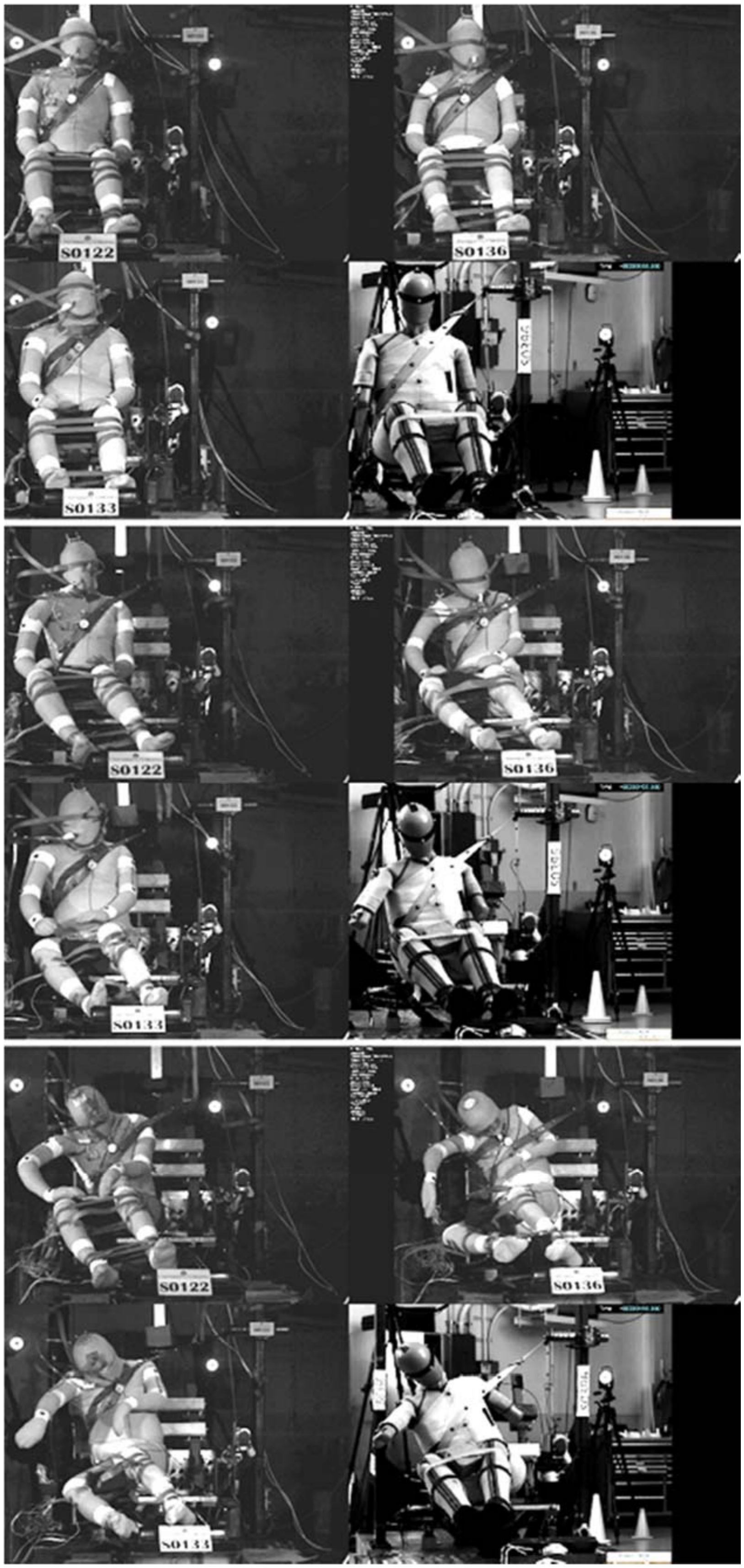

Fig. C-1. ATD and PMHS response in configuration 1 at 50 ms (up), 100 ms (centre) and 150 ms (down).

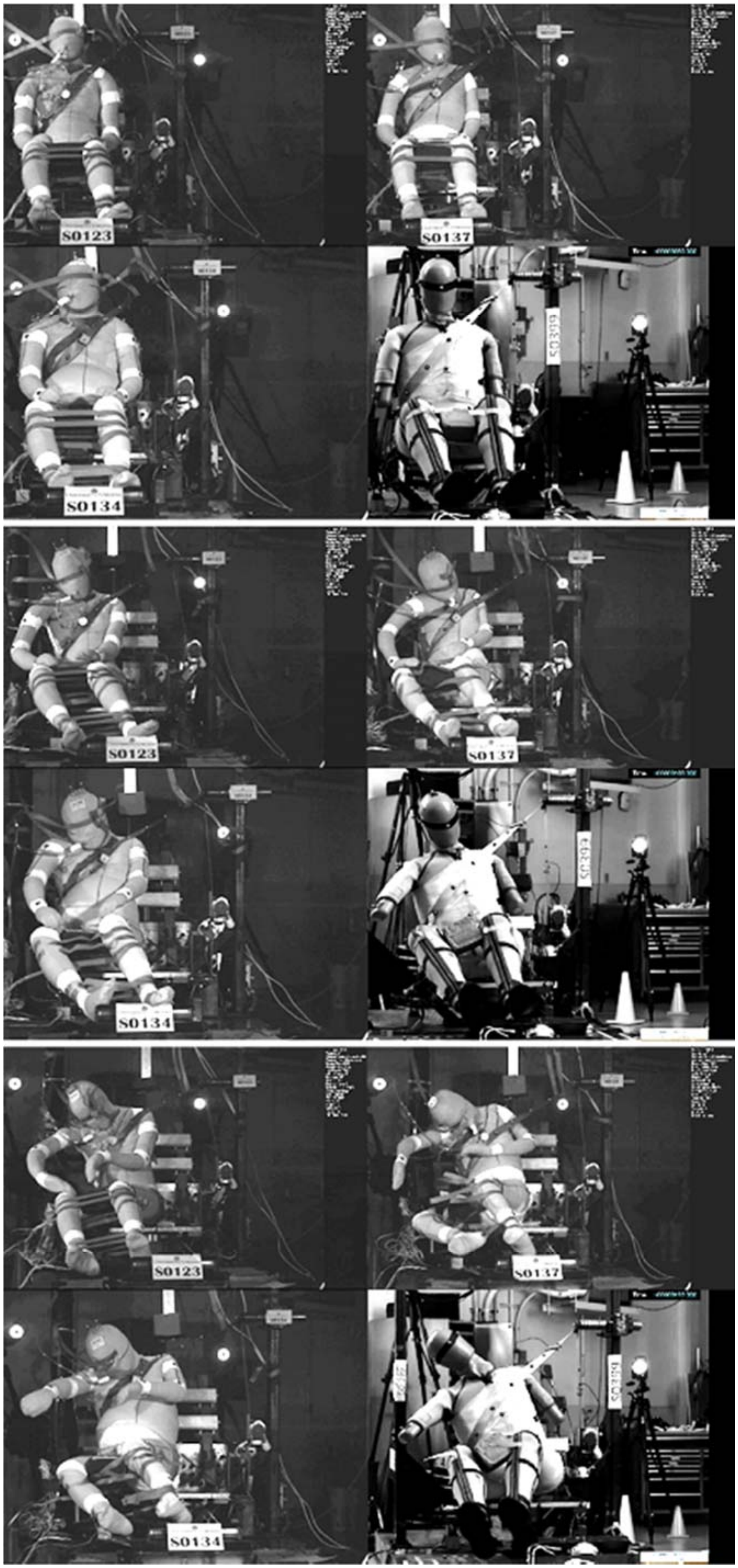

Fig. C-2. ATD and PMHS response in configuration 2 at 50 ms (up), 100 ms (centre) and 150 ms (down).

Fig. C-3. ATD and PMHS response in configuration 3 at 50 ms (up), 100 ms (centre) and 150 ms (down).

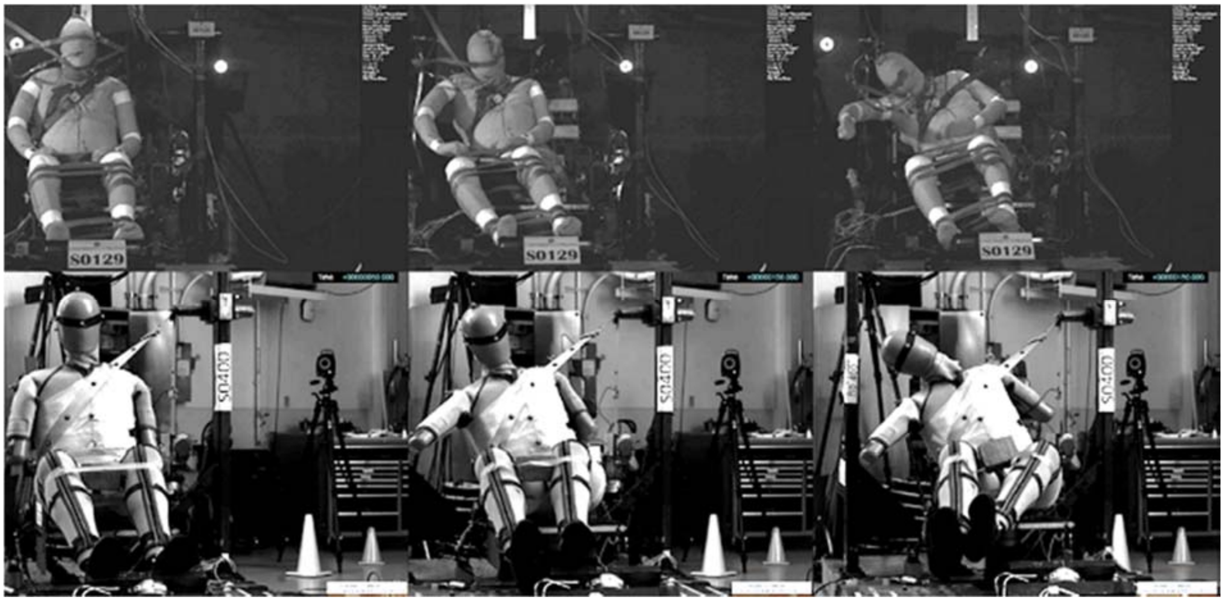

Fig. C-4. ATD and PMHS response in configuration 4 at 50 ms (left), 100 ms (centre) and 150 ms (right).

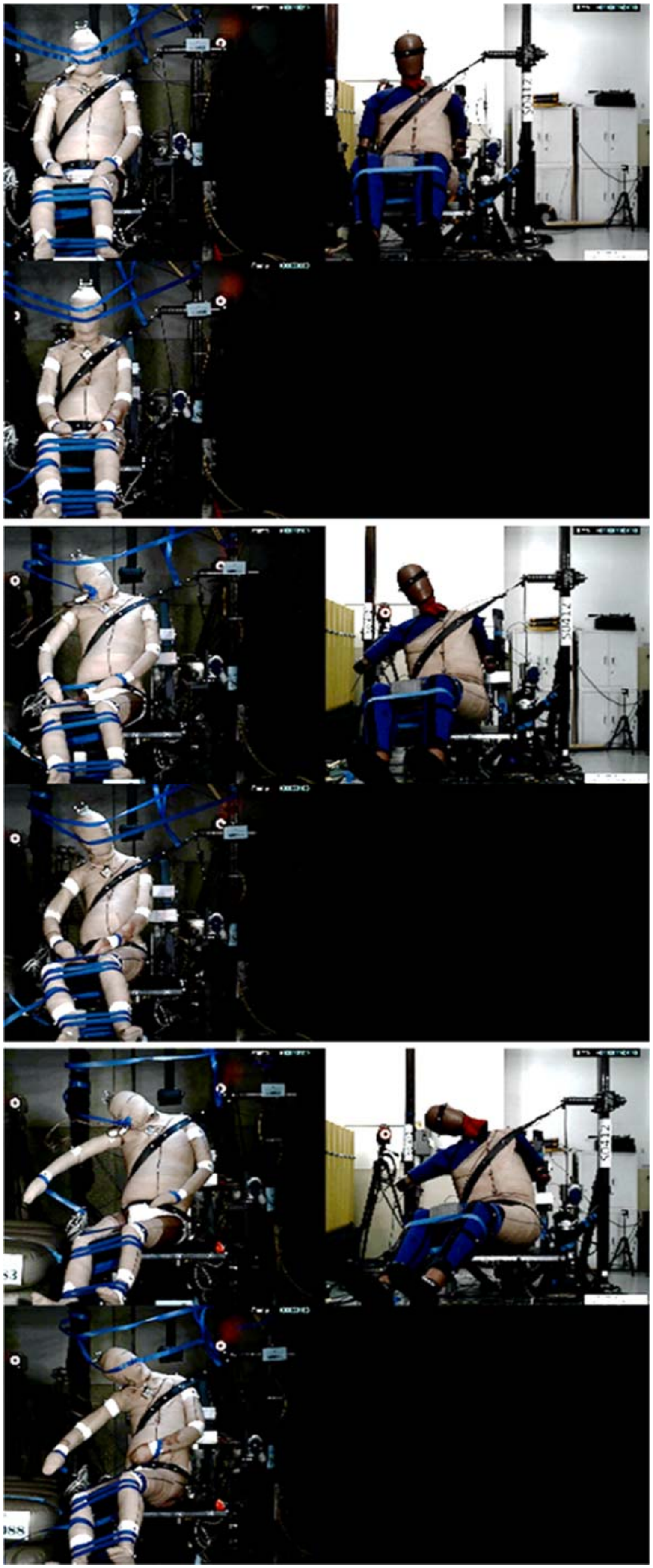

Fig. C-5. ATD and PMHS response in configuration 5 at 50 ms (up), 100 ms (centre) and 150 ms (down).

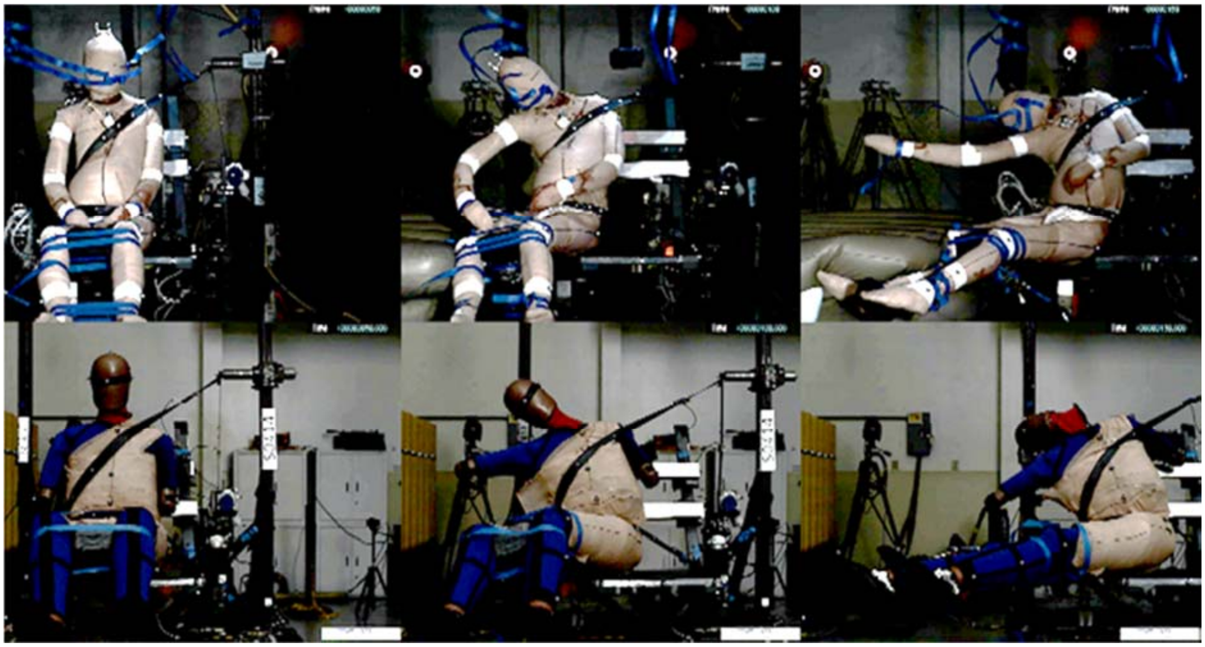

Fig. C-6. ATD and PMHS response in configuration 6 at 50 ms (left), 100 ms (centre) and 150 ms (right).